Environmental Science & Technology

pubs.acs.org/est

Article

Multiple Pathways Drive CH_4 and N_2O Emissions in Coastal Macroalgal Ecosystems

Hongmei Li,[¶] Xiaojie Wang,[¶] Yue Tian,[¶] Xianhui Wan, Liyang Zhan,* Zenghu Zhang, Yihua Xiao, and Yongyu Zhang*

Cite This: https://doi.org/10.1021/acs.est.5c18290

Read Online

ACCESS | Metrics & More | Article Recommendations | Supporting Information

ABSTRACT: Coastal macroalgal ecosystems, while recognized for their capacity to sequester CO_2, remain poorly understood as potential sources of potent greenhouse gases methane (CH_4) and nitrous oxide (N_2O). Here, we show that the surface waters dominated by *Ulva prolifera* during green tide in the Yellow Sea exhibited 346% and 147% higher CH_4 and N_2O concentrations, respectively, compared to nonmacroalgal waters, despite dissolved oxygen (DO) levels exceeding 6.0 mg/L. Laboratory cultivation experiments revealed a two-stage dynamic of CH_4 release: during the growth stage (DO > 5.0 mg/L), CH_4 release was driven primarily by algal photosynthesis and reactive oxygen species; whereas during decay (DO > 4.0 mg/L), CH_4 release increased 2−3 fold, fueled by microbial degradation of algal-derived methanogenic precursors, including dimethylsulfoniopropionate and methylphosphonate. Methanogenic archaea were also detected in anoxic microniches within the macroalgal matrix, indicating additional CH_4 production. For N_2O, isotopic tracing experiment demonstrated that both ammonia oxidation and denitrification contribute to its production during macroalgal growth, while emissions declined to negligible levels during late decay due to nitrogen depletion. These findings reveal multiple aerobic pathways for CH_4 and N_2O emissions in coastal macroalgal ecosystems, highlighting previously unrecognized non-CO_2 greenhouse gas fluxes that should be considered alongside carbon sequestration in evaluating the climate impacts of macroalgae.

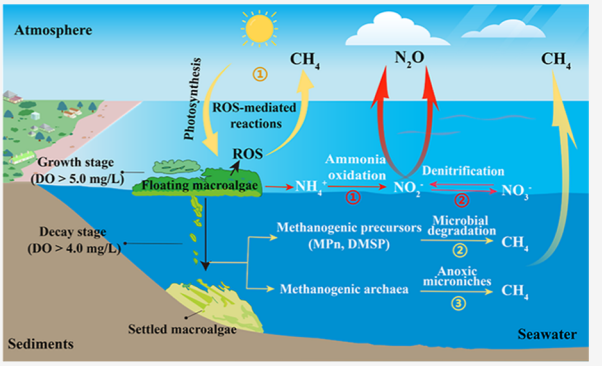

KEYWORDS: *macroalgae, Ulva prolifera, aerobic methanogenesis, nitrous oxide production, climate regulation*

1. INTRODUCTION

Methane (CH_4) and nitrous oxide (N_2O), the second and third most potent greenhouse gases after carbon dioxide (CO_2), possess global warming potentials of 27 and 270 times greater than CO_2 over a 100-year time frame.[1,2] Their atmospheric concentrations have surged alarmingly since the preindustrial era (CH_4: + 161%; N_2O: + 23%), with the marine systems representing significant sources of CH_4 and N_2O to the atmosphere.[3,4] Coastal vegetated ecosystems dominated by seagrass meadows, mangrove forests, and saltmarshes are recognized as hotspots for CH_4 and N_2O emissions due to methanogenic fermentation in anoxic sediments and anthropogenic nitrogen (N) loading.[5,6] Nevertheless, the release of CH_4 and N_2O by macroalgae, the most productive coastal macrophytes, remains poorly understood as they thrive primarily in oxygenated waters where conventional anaerobic production mechanisms are suppressed.

Under the context of carbon neutrality, macroalgae have attracted increasing attention for their capacity to sequester carbon through sedimentary burial of macroalgal particulate organic carbon (POC), release of macroalgal recalcitrant dissolved organic carbon (RDOC), and their export to the deep ocean.[7−10] However, their prevalence in oxygenated environments raises a critical question: could macroalgae represent previously overlooked sources of CH_4 and N_2O under aerobic conditions? This knowledge gap profoundly impacts the holistic assessment of macroalgae's net climate regulation effects. Conventional understanding attributes CH_4 production strictly to anaerobic environments, but recent observations of CH_4 supersaturation in oxygenated surface waters, termed the "marine methane paradox", have challenged this paradigm.[11−13] For instance, significant CH_4 emissions have been reported from sedimentary macroalgal ecosystems in the Baltic Sea, which were primarily driven by methanogenic archaea in anoxic microenvironments.[14] Beyond such cryptic anoxic niches,[15] several aerobic CH_4 production pathways have been proposed, including: (i) reactive oxygen species (ROS)-

Received: December 17, 2025
Revised: March 4, 2026
Accepted: March 4, 2026
Published: March 13, 2026

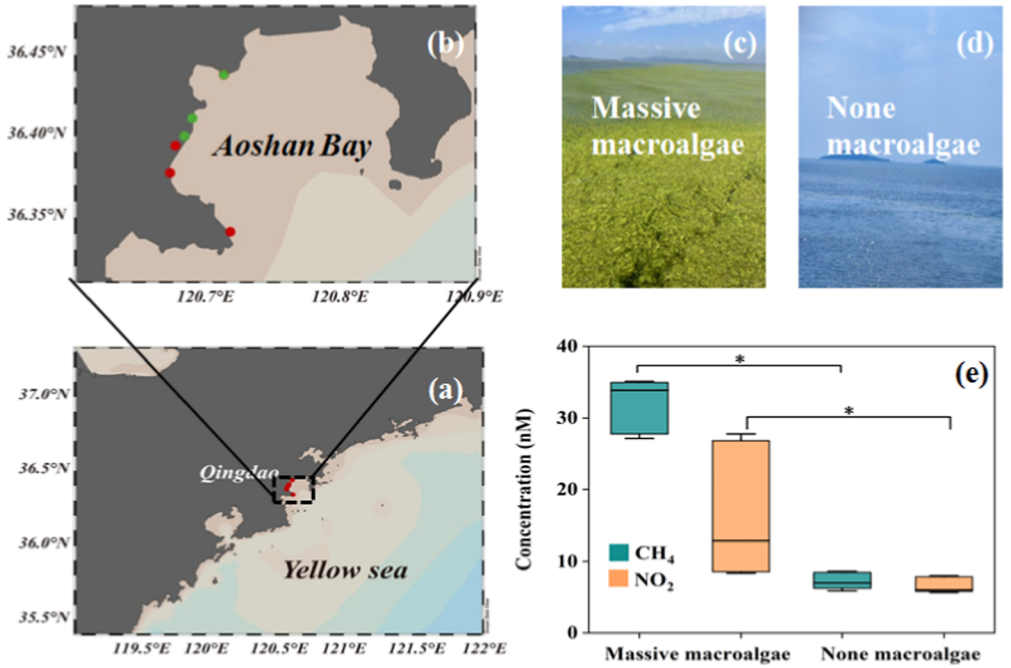

Figure 1. (a,b) Area maps with field sampling sites. The green and red circles represent sampling sites with massive and none macroalgae in the coastal waters of Qingdao, respectively. (c,d) Regions covered by massive and none macroalgae, respectively. (e) Concentrations of CH_4 and N_2O in massive- and none-macroalgae areas during the macroalgal bloom, respectively.

mediated demethylation of methylated compounds such as dimethylsulfoniopropionate (DMSP) and dimethylsulfoxide (DMSO);[16,17] (ii) bacterial cleavage of methylphosphonates (MPn) in phosphorus-limited waters;[18,19] and (iii) activity of aerotolerant methylotrophic methanogens in oxygenated sediments.[20] Despite these advances, the pathways and mechanisms driving CH_4 production in buoyant, photosynthetic macroalgae growing in oxygenated surface waters remain unclear. Macroalgae release substantial amounts of organic matter during growth and decay, providing sufficient energy for marine microorganisms.[21,22] However, it is unclear whether CH_4 arises as a byproduct during microbial degradation of macroalgae-derived organic matter, or is produced directly through macroalgal physiological processes.

Equally unknown is N_2O release from macroalgae under aerobic condition. Although ammonia oxidation dominates aerobic N_2O production,[23] emerging evidence suggests that cryptic denitrification hotspots can form in anoxic microenvironments associated with particulate organic matter.[24,25] We therefore hypothesize that macroalgal canopies may promote N_2O through (1) exudation of labile organic matter that stimulates nitrifying and denitrifying microorganisms[26] and (2) accumulated algal detritus and POC creating localized anoxia that supports denitrification.[12,27] These mechanisms may be especially relevant under anthropogenic N loading,[28] but direct evidence from macroalgal systems is lacking.

Indeed, macroalgae undergo dynamic physiological changes throughout their life cycle. Photosynthesis dominates early growth stages and elevates dissolved oxygen (DO) concentrations, while microbial respiration and degradation prevail during senescence and significantly deplete DO levels.[29] Currently, CH_4 and N_2O release by macroalgae at different growth stages and their production mechanisms remain underexplored. Here, we address these gaps through integrated field and laboratory studies. Using *Ulva prolifera*, a globally relevant buoyant macroalgae responsible for the world's largest macroalgal blooms (green tides) in the Yellow Sea, we quantified in situ CH_4 and N_2O release at different algal densities, and elucidated their production mechanisms during growth and decay stages through a series of laboratory cultivation experiments. Our findings demonstrate that macroalgae as previously unrecognized sources of CH_4 and N_2O in aerobic environments, reveal distinct stage-dependent production processes, and highlight the importance of accounting for these emissions when evaluating the net climate-regulation functions of macroalgal ecosystems.

2. MATERIALS AND METHODS

2.1. Field Investigation during the Macroalgal Blooms

A field survey was conducted during the late stage of a green tide (July 20−21, 2023) in coastal waters of Qingdao, South Yellow Sea (Figure 1a,b). Six sampling sites were strategically selected, including three sites with massive *U. prolifera* biomass (i.e., massive-macroalgae area) and three control sites without *U. prolifera* (i.e., none-macroalgae area) (Figure 1c,d). Surface water samples were collected using a custom sampler for the analysis of CH_4, N_2O, DOC, POC, dissolved inorganic carbon (DIC), dissolved inorganic nitrogen (DIN = NO_3^- (nitrate) + NO_2^- (nitrite) + NH_4^+ (ammonium)), phosphate (PO_4^{3-}) and microbial abundance. Meanwhile, hydrological parameters, including temperature (T), salinity (S), DO and pH were recorded in situ using a multiparameter water quality analyzer (YSI EXO2Multiparameter Sonde, USA). Seawater samples for CH_4 and N_2O analysis were collected in 100 mL serum bottles and filled smoothly from the bottom using silicone tubing, which were overflowed two to three times its volume to avoid any contamination from air. Then 90 μL of saturated $HgCl_2$ solution was added, and the bottle was immediately secured with a butyl rubber stopper and aluminum cap. Triplicate samples were stored in a dark box at 4 °C. Further details on sample collection are provided in the Supporting Information (Section S3.1).

https://doi.org/10.1021/acs.est.5c18290
Environ. Sci. Technol. XXXX, XXX, XXX−XXX

2.2. Laboratory Experiments: Dynamics and Production Mechanisms of CH_4 and N_2O Release by *U. prolifera*

To explore the dynamics of CH_4 and N_2O release by macroalgae, *U. prolifera* (sampled at the late-bloom stage) was cultivated in 12-L transparent polycarbonate tanks under controlled conditions (20 °C, 50 μmol photons·m^{-2}·s^{-1}, 12:12 light−dark cycle). Three algal density treatments (1, 5, and 10 g *fw*/L; *fw* = fresh weight) were established in 10 L of 3-μm filtered natural seawater amended with f/2 inorganic nutrients, while algae-free tanks were served as controls (n = 3 per group). Over an 18-day incubation, water samples were collected on days 0, 1, 2, 3, 5, 7, 10, and 18 for analysis of CH_4, N_2O, DOC, POC, DIC, DIN and PO_4^{3-}. Seawater DO was concurrently measured using a calibrated WTW TetrCon925 probe. The physiological status of *U. prolifera* was monitored daily via chlorophyll fluorescence (F_v/F_m) to divide the cultivation into growth and decay stages. During the incubation, all tank ports were covered with 0.2-μm pore-size membranes to maintain atmospheric exchange while minimizing contamination. Following each sampling, sterile artificial seawater was replenished postsampling to maintain constant volume.

To further elucidate the production mechanisms of CH_4 and N_2O by macroalgae, a series of complementary incubation experiments were conducted. (1) Diurnal dynamics and influence of photosynthesis and ROS: *U. prolifera* (10 g *fw*/L) was continuously cultivated for 48 h under 12h:12h light/dark cycles to examine diurnal variations in CH_4 and N_2O release and assess the influence of photosynthesis and ROS on CH_4 production. Treatments (with macroalgae) and controls (without macroalgae) were established. CH_4 and N_2O concentrations, along with ROS content were monitored at 2-h intervals. DMSP lyase activity was concurrently measured to exclude potential contributions of microorganisms to diurnal CH_4 variations by degrading methanogenic precursors. (2) Effects of nitrogen (N) and phosphorus (P) concentrations: (i) N influence: Given that NO_3^- is the major form of N nutrients in South Yellow Sea,[30] *U. prolifera* (3 g *fw*/L) was cultivated for 25 days under two different initial NO_3^- concentrations (20 μM vs 40 μM) to assess the influence of N on CH_4 and N_2O emissions, with PO_4^{3-} concentration unified to 1.25 μM. Meanwhile, to trace N_2O production pathways (ammonia oxidation vs denitrification), parallel incubations were performed using different ^{15}N-tracers as the sole N sources: $^{15}NH_4Cl$ (99% ^{15}N, Yuanye) and $Na^{15}NO_3$ (98% ^{15}N, Sigma), with initial N concentration of 40 μM (^{15}N fraction of 10%) and PO_4^{3-} of 2.50 μM. (ii) P influence: to investigate whether macroalgae release MPn (a potential methanogenesis precursor) and whether microorganisms utilize MPn for methanogenesis under PO_4^{3-} limitation, *U. prolifera* was cultivated under different initial PO_4^{3-} (NaH_2PO_4) concentrations (1.25 μM vs 0.56 μM; NO_3^- = 20 μM). Dissolved organic phosphorus (DOP) concentration and C−P lyase activity were measured concurrently. For all nutrient influence experiments, control tanks containing seawater with same N or P nutrients but lacking *U. prolifera* were included. Water samples were collected on days 0, 1, 3, 5, 7, 10, and 25 for analysis of CH_4, N_2O, $\delta^{15}N$ of N_2O, DOC, POC, DIC, DIN, PO_4^{3-}, and microbial abundance. Seawater DO was measured using a calibrated WTW TetrCon925 probe. (3) Detection of anoxic microniches: To determine whether anoxic microniches exist within the macroalgal matrix, DO horizontal profiles within the matrix were measured on day 7 (3 g *fw*/L), corresponding to the point of lowest recorded seawater DO (~4.0 mg/L). Moreover, to further assess the influence of macroalgal density on microniche formation, DO concentrations were measured at three defined horizontal distances from the matrix outside (5 cm, 2.5 cm, and 2.5 mm inward) on day 18 during cultivation of *U. prolifera* at different biomass densities (1, 5, and 10 g *fw*/L). (4) Microbial community analysis: To characterize microbial contributions to CH_4 and N_2O productions, samples for analyzing microbial community composition were collected on days 0, 5, 9, and 25. All culture conditions were the same as in previous experiments.

2.3. Sample Analysis

2.3.1. Concentration of CH_4 and Different Forms of Carbon. CH_4 concentrations were measured using an Agilent 7890A gas chromatograph equipped with a flame ionization detector (FID), which were extracted from the subsamples by a purge-and-trap method prior to analysis.[31] DOC concentrations were measured using a TOC-L analyzer equipped with an ASI-V autosampler (Shimadzu, TOC-L CPH, Japan).[32] POC concentrations were measured using Series II CHNS/O Analyzer (PE2400, USA).[22] DIC concentrations were measured using a DIC analyzer equipped with an infrared CO_2 detector (AS-C3; Apollo SciTech Inc., USA).[29]

2.3.2. Concentration and Isotope of N_2O. Concentrations and isotopes of N_2O were measured using a modified GC-IRMS with large volume purge and trap system.[3] The precision of this method was estimated to be better than ±3%. The precision of $\delta^{15}N$ measurements with 2 nmol N_2O reference gas was better than 0.3‰.

2.3.3. Concentration of Nutrients. Concentrations of NO_3^-, NO_2^-, NH_4^+, PO_4^{3-} and DOP were determined using an AutoAnalyzer (BRAN & LUEBBE AA3, Germany).[33] Based on previous studies indicating that phosphonates account for ~21% of DOP in natural seawater,[18] and that ~31% of phosphonates have a C−P structure similar to MPn, the MPn concentration was estimated as 6.51% of the measured DOP concentration.[11]

2.3.4. ROS Content and Enzymatic Activity Determination. The ROS content in *U. prolifera* was quantified fluorometrically using H_2O_2 as a proxy. Fresh algal fronds (1.0 g) were ground into powder and treated with 0.05 M phosphate-buffered saline (PBS). Following centrifugation and dark incubation, ROS content was determined via microplate reader (excitation, 488 nm; emission, 53 nm; Infinite M200 Pro; Tecan, Switzerland).[34] The activities of DMSP lyase and C−P lyase were determined using reagent kits (Wuhan adanti Biotechnology Co., Ltd.) based on a phosphorylation-specific antibody capture mechanism. The assays employ antibodies coated onto microplates to specifically recognize phosphorylated amino acid residues, thereby reflecting enzyme activity.

2.3.5. DO Horizontal Profile Measurement. The DO horizontal profile within the macroalgal matrix was measured via voltammetric analysis using an electrochemical workstation (AutoLab PGSTAT10, Metrohm, Switzerland).[35] A microelectrode was deployed from the outside into the matrix interior in 0.5 mm increments using a micromanipulator.

2.3.6. Microbial Abundance and Microbial Community Composition. Microbial abundance was measured using an Accuri II flow cytometer (BD Biosciences) after staining with SYBR Green I (Invitrogen, United Kingdom). The microbial community composition was determined using 16S rRNA gene sequencing, using bacterial primer set 338F/806R[36] and archaeal primer set Arch519F/Arch915R[37] for amplification, followed by sequencing on the Illumina MiSeq platform.

Details of concentrations of CH_4, N_2O, isotopic analyses of N_2O, different forms of carbon, nutrients, ROS content, enzymatic activity assays, DO depth profiles, and microbial community composition analysis are provided in Supporting Information (Section S3.2).

2.4. Calculation of CH_4 and N_2O Fluxes by Macroalgae

The fluxes (F, mg·m^{-2}·d^{-1}) of CH_4 and N_2O by macroalgae to the atmosphere were estimated as follows

$$F = k \times (C_{me} - C_{eq}) \quad (1)$$

where C_{me} (nM) represents the measured concentrations of CH_4 and N_2O dissolved in seawater, and C_{eq} (nM) represents the concentrations in equilibrium with the partial pressures of CH_4 and N_2O in the atmosphere. The C_{eq} for CH_4 is calculated using the temperature, salinity, and solubility of seawater during cultivation,[38] whereas the C_{eq} for N_2O is calculated using the current atmospheric N_2O mixing ratios and the temperature and salinity of seawater during cultivation.

k is the gas transfer velocity (cm·h^{-1}), which is estimated based on the wind speed (U = 3 m·s^{-1}) during cultivation and the Schmidt number (Sc). It was calculated as follows

$$k = 0.251 \times U^2 \times (Sc/660)^{-0.5} \quad (2)$$

https://doi.org/10.1021/acs.est.5c18290
Environ. Sci. Technol. XXXX, XXX, XXX−XXX

where *Sc* is the Schmidt number, which is determined by the temperature, salinity and gas molecular properties of seawater during cultivation.[39,40]

2.5. Statistical Analysis

In this study, statistical assumptions of normality and homogeneity of variance were evaluated prior to group comparisons. As the data violated the assumption of homoscedasticity required for standard one-way ANOVA, Welch's ANOVA was applied to ensure robust comparison among groups with unequal variances. All analyses were conducted at a significance level of $\alpha = 0.05$ using SPSS (version 28.0).

Moreover, clustered heatmaps were performed to visualize the relationships between CH_4 and N_2O concentrations and environmental parameters (macroalgal biomass, *T*, S, DO, pH, DIN and PO_4^{3-}). Pairwise Pearson correlation coefficients (r) were calculated for all variables. The correlation matrix was visualized as a hierarchically clustered heatmap using the "pheatmap" package in R (v4.3.1), applying Euclidean distance and complete linkage to both dimensions.

3. RESULTS

3.1. Elevated CH_4 and N_2O Concentrations in Massive-Macroalgae Area

During the macroalgal bloom, surface seawater in the massive-macroalgae area showed elevated concentrations of CH_4 (32.1 ± 3.5 vs 7.2 ± 1.1 nM; $p < 0.05$, Welch's ANOVA) and N_2O (16.3 ± 8.6 vs 6.6 ± 1.0 nM; $p < 0.05$, Welch's ANOVA) compared to none-macroalgae area (Figure 1e), representing increases of 346% and 147%, respectively. Meanwhile, elevated levels of DOC, POC, DIC and microbial abundance were observed in massive-macroalgae area (Table S1). Heatmap analysis revealed strong positive correlations between macroalgal biomass and CH_4 ($r = 0.953$) and N_2O concentrations ($r = 0.732$; Figure S1), surpassing the influence of other environmental variables (i.e., T, S, DO, pH, DIN and PO_4^{3-}). These results suggest that macroalgae bloom stimulates CH_4 and N_2O production and emission compared to the none-macroalgae area.

3.2. CH_4 and N_2O Release by Macroalgae at Different Stages

According to the changes in F_v/F_m of *U. prolifera*, the cultivation of macroalgae was divided into growth (Days 0–5, F_v/F_m increase) and decay stages (Days 5–18, F_v/F_m decline to 0; Figure S2a). The CH_4 release occurred throughout both stages and intensified during decay, with concentrations being 2–3 times higher than those during growth (Figure 2a). Meanwhile, DOC, POC and DIC levels progressively increased from growth to decay (Figure S3a–c). In contrast, N_2O concentrations exhibited an inverse trend, peaking during growth and becoming negligible during late decay (Figure 2b). Both CH_4 and N_2O concentrations increased with algal biomass density, reinforcing macroalgae-dependent release patterns.

3.3. Influence of Photosynthesis and ROS on CH_4 and N_2O Release by Macroalgae

The 48-h diurnal monitoring revealed distinct light-mediated patterns of CH_4 and N_2O release. CH_4 concentrations were significantly higher during light periods than those during dark periods (25.4 ± 7.5 nM vs 11.4 ± 3.5 nM; $p < 0.001$, Welch's ANOVA; Figure 3a). This light-dependent increase coincided with elevated ROS levels during the day (Figure S4), and a significant correlation was observed between ROS content and CH_4 concentrations ($\rho = 0.66$, $p < 0.0001$, Spearman correlations; Figure S5), collectively suggesting that photosynthesis and ROS facilitate CH_4 production. In contrast, N_2O concentrations decreased progressively and were irrespective of light cycles (Figure 3b), implying light-independent mechanisms of N_2O production.

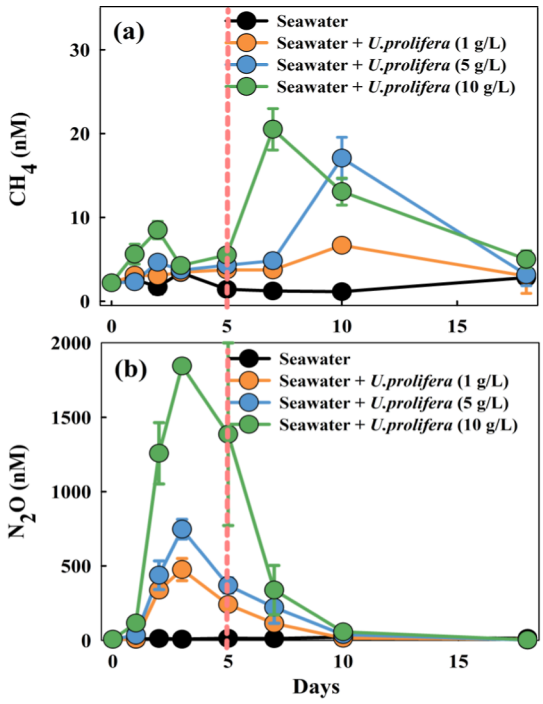

Figure 2. Dynamic changes in CH_4 (a) and N_2O (b) concentrations at different stages during the cultivation of *U. prolifera*.

3.4. Effect of N and P Concentrations on CH_4 and N_2O Production by Macroalgae

Consistent with prior experiments, cultivations under different N and P conditions were also divided into growth (0–5 days) and decay (5–25 days) stages according to the changes in F_v/F_m of *U. prolifera* (Figure S2b). In the treatments with different NO_3^- additions (20 μM vs 40 μM), CH_4 concentrations increased with lower NO_3^- availability (Figures 4a and S6d), suggesting enhanced CH_4 accumulation under *N*-deficient conditions (associated with accelerated algal decay). Conversely, N_2O concentrations increased with elevated NO_3^- (Figures 4b and S6d), suggesting high *N*-stimulated N_2O production. Isotopic tracing experiment identified $^{15}N_2O$ production in both $^{15}NH_4Cl$ and $Na^{15}NO_3^-$ amended treatments (Figure 5), indicating that both ammonia oxidation and denitrification contribute to N_2O production. $^{15}N_2O$ concentration in the $^{15}NO_3^-$ treatment was higher during growth stage and decreased toward decay stage, while $^{15}N_2O$ concentration in the $^{15}NH_4^+$ treatment showed a more stable production rate throughout the incubation, implying a stage-specific N_2O source structure. Notably, the peak $^{15}N_2O$ concentration was observed in the $^{15}NO_3^-$ treatment during the growth stage, suggesting active denitrification contributes to N_2O production despite the high ambient DO concentration.

In contrast to N effects, P availability distinctly influenced CH_4 but not N_2O production. Under P-limited conditions (0.56 μM PO_4^{3-}), CH_4 concentrations increased compared to high P supply (1.25 μM PO_4^{3-}; Figures 4c and S7a). We concurrently observed a more rapid decrease in MPn

https://doi.org/10.1021/acs.est.5c18290
Environ. Sci. Technol. XXXX, XXX, XXX−XXX

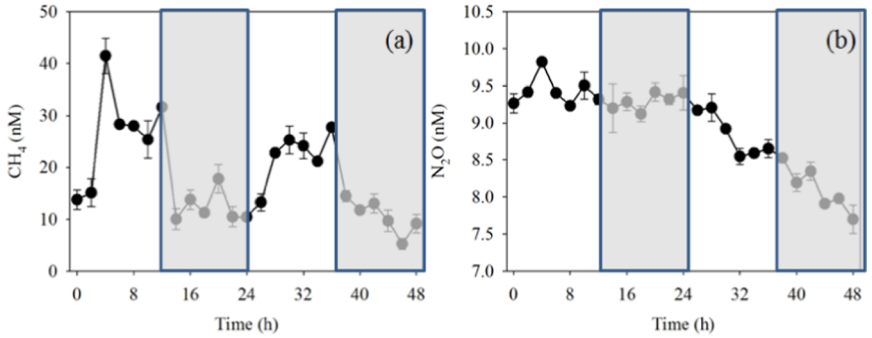

Figure 3. Dynamic changes in CH_4 (a) and N_2O (b) concentrations during the 48-h continuous cultivation under different light conditions. White background indicates light (daytime) condition, while gray background indicates dark (nighttime) condition.

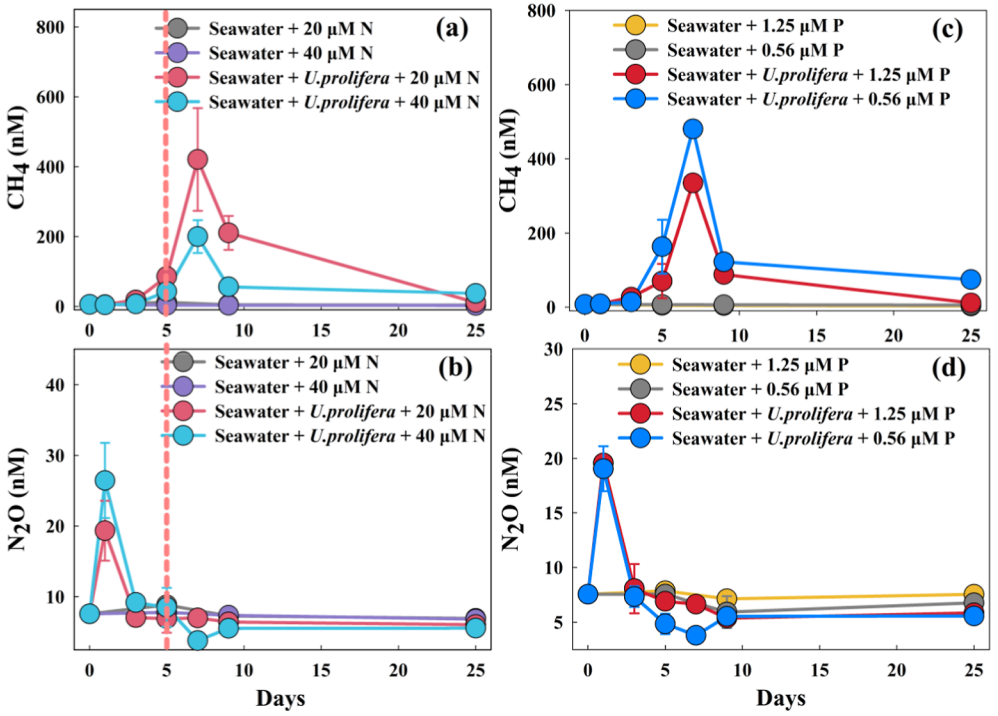

Figure 4. Dynamic changes in CH_4 (a,c) and N_2O (b,d) concentrations during the cultivation of *U. prolifera* under different N (NO_3^-, a,b) and P (PO_4^{3-}, c,d) additions.

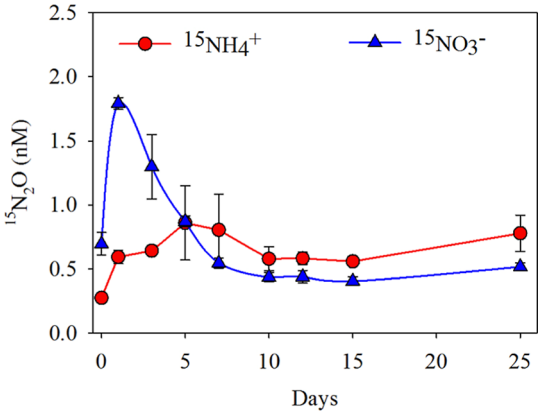

Figure 5. Dynamic changes in $^{15}N_2O$ concentrations during the cultivation of *U. prolifera* using $^{15}NH_4^+$ and $^{15}NO_3^-$.

concentration under PO_4^{3-}-deficient conditions (Figure S7b), suggesting potential microbial utilization of organic phosphorus for methanogenesis. By contrast, N_2O remained unaffected across the phosphorus gradient (Figure 4d).

3.5. Microbial Contributions to CH_4 and N_2O Production Associate with Macroalgae

To elucidate the role of microorganisms in CH_4 and N_2O production by macroalgae, we characterized microbial abundance and community composition during the cultivation with different NO_3^- additions. Microbial abundance exhibited bimodal dynamics consistent with the growth (0−5 days) and decay (5−25 days) stages (Figure S8). Concurrently, microbial community composition underwent significant stage-dependent succession (Figures 6 and S9). Bacteria specialized in organic carbon decomposition (e.g., *Bacteroidia* and *Clostridia*) showed a continuous increase from growth to decay (Figure 6a). Notably, genera implicated in methanogenesis via precursor utilization (e.g., *unclassified_f_Rhodobacteraceae* and *Pseudophaeobacter*) peaked during decay (Figure 6b). In contrast, taxa associated with denitrification (e.g., Saprospiraceae, Arcobacteraceae, Nitrincolaceae) showed relatively higher abundance during growth (Figure S9). Moreover,

https://doi.org/10.1021/acs.est.5c18290
Environ. Sci. Technol. XXXX, XXX, XXX−XXX

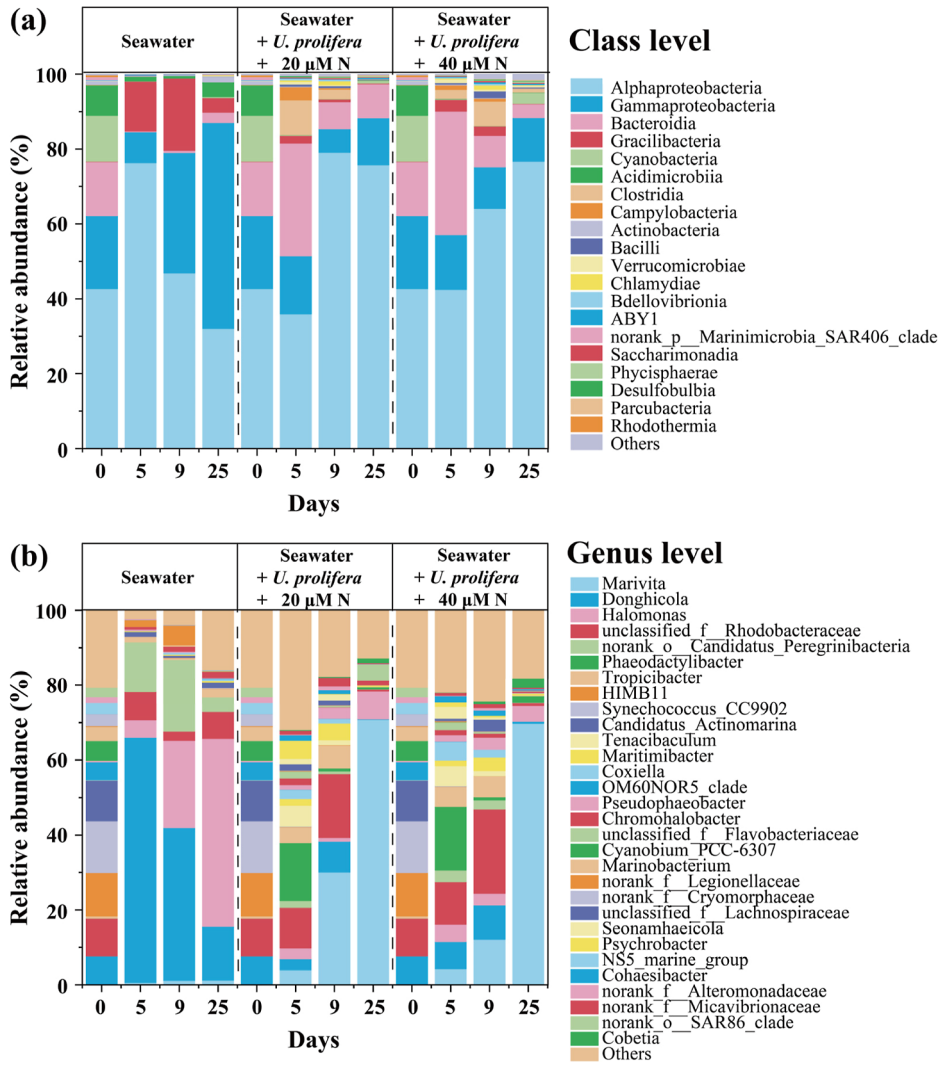

Figure 6. Dynamic changes in microbial community structure during the cultivation of *U. prolifera* under different N (NO_3^-) conditions. (a) Microbial community structure at the class level; (b) microbial community structure at the genus level.

methanogenic archaea (*Methanolobus*, *Methanobacterium*, *Methanobrevibacter*, *Methanosaeta*, *Methanosarcina*; Figure S10a) and ammonia-oxidizing archaea (uncategorized *Nitrosopumilaceae*, *Nitrososphaeraceae*, *Nitrosotaleaceae*; Figure S10b) were observed in the treatments with *U. prolifera*. As for the groups with different NO_3^- additions, N_2O production genera (*Seonamhaeicola* and *Cohaesbacter*) showed higher relative abundance under high NO_3^- conditions (40 μM vs 20 μM) (Figure 6b).

3.6. CH_4 and N_2O Fluxes by *U. prolifera*

According to eqs 1 and 2, the CH_4 and N_2O fluxes by *U. prolifera* were calculated under simulated in situ conditions, with a biomass density of 3 g/L, NO_3^- concentration of 20 μM, and PO_4^{3-} concentration of 1.25 μM, consistent with typical field observations.[41,42] After calculation, the daily fluxes of CH_4 and N_2O released by *U. prolifera* were 3.8 ± 1.3 mg m^{-2} d^{-1} and 0.13 ± 0.06 mg m^{-2} d^{-1}, respectively (Figure 7).

4. DISCUSSION

Although macroalgal carbon sequestration represents a critical natural process for mitigating atmospheric CO_2 through long-term marine carbon storage,[43,44] its net climate benefit is potentially compromised by coemission of the potent greenhouse gases CH_4 and N_2O. However, little is known about these emissions so far. This study advances the objective assessment of macroalgae's climate regulation potential by elucidating the aerobic methanogenesis pathway and deciphering coupled nitrification and denitrification processes driving N_2O production in buoyant macroalga *U. prolifera*.

Our field observations revealed significantly elevated CH_4 and N_2O concentrations ($p < 0.05$) in surface seawater beneath *U. prolifera* mats during the late stage of green tide compared to none-macroalgae waters (Figure 1). Heatmap analysis identified macroalgal biomass as the principal driver of CH_4 and N_2O accumulation (Figure S1), supporting our hypothesis that *U. prolifera* releases copious amounts of CH_4 and N_2O during both growth and early decay. Notably, DO levels remained aerobic in both massive-macroalgae (6.1 ± 0.5 mg/L) and none-macroalgae waters (6.4 ± 0.1 mg/L, Table S1), challenging the conventional paradigm of anaerobic methanogenesis and implicating alternative aerobic CH_4 production mechanisms.

Laboratory cultivation experiments further demonstrated persistent CH_4 release throughout both growth and decay stages of *U. prolifera*, with decay-stage fluxes exceeding growth-

https://doi.org/10.1021/acs.est.5c18290
Environ. Sci. Technol. XXXX, XXX, XXX−XXX

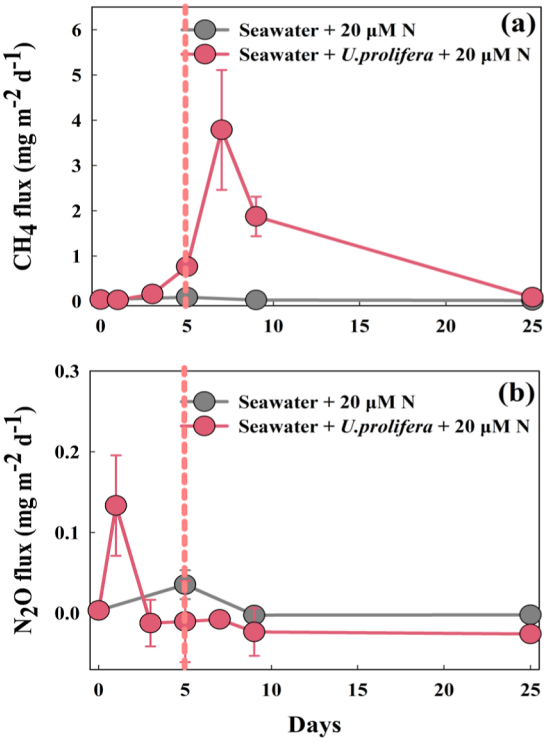

Figure 7. Dynamic changes in CH_4 (a) and N_2O (b) fluxes during the cultivation of *U. prolifera* with biomass density of 3 g/L under 20 μM NO_3^- and 1.25 μM PO_4^{3-}.

stage release by 2−3 folds (Figures 2a and S11a). Critically, though DO concentrations varied, it was consistently above 4.0 mg/L during both stages (Figure S12a), thus precluding conventional anoxic methanogenesis as the primary pathway. We thus propose three potential mechanisms for aerobic CH_4 production in macroalgae:

Photosynthesis and ROS-driven methanogenesis: During the 48-h continuous cultivation, daytime CH_4 release from *U. prolifera* was significantly higher than nighttime emissions ($p < 0.001$, Figure 3a), demonstrating light-dependent regulation of methanogenesis. Photosynthetically derived ATP provides energy for the biosynthesis of methylated sulfur compounds, such as dimethylsulfoniopropionate (DMSP) and dimethylsulfide (DMS), which serve as precursors for CH_4 generation via microbial or ROS-mediated demethylation.[16,45−47] Importantly, DMSP is synthesized within macroalgal cells through well-characterized metabolic pathways (e.g., transamination and decarboxylation), implying that macroalgae themselves are a potential source of these methanogenic precursors.[48,49] Meanwhile, ROS levels exhibited clear diurnal variations (daytime > nighttime, Figure S4) and were significantly correlated with CH_4 concentrations ($p < 0.0001$, Figure S5), suggesting that photosynthesis and ROS synergistically drive methanogenesis. This aligns with emerging evidence for a ubiquitous nonenzymatic CH_4 production pathway driven by ROS-iron-methyl donor interactions in living cells.[16] In iron-rich environments, ROS can initiate Fenton reactions that methionine (DMSP precursor) and thioethers (DMSP cleavage products) undergo demethylation to produce CH_4.[16,17,50] The absence of diurnal variation in DMSP lyase activity (Figure S13) further precludes substantial microbial DMSP degradation as the main driver of the observed diurnal CH_4 fluctuations. Studies on other marine algal species have shown that both CH_4 production and photosynthetic O_2 evolution cease upon addition of photosynthetic inhibitors, providing additional evidence that algae themselves contribute to CH_4 production during photosynthesis.[17,51] A recent review similarly proposed that macroalgae directly contribute to oxic CH_4 production through the release of methylated compounds that serve as CH_4 precursors.[52] Together, these converging lines of evidence establish light-dependent, ROS-mediated CH_4 production as a major pathway of aerobic methanogenesis during macroalgal growth.

Microbial degradation of macroalgae-derived methanogenic precursors: Beyond the ROS-driven nonenzymatic pathway, aerobic bacterial metabolism of DMSP via DMSP lyase also contributes to CH_4 production.[46] Indeed, *U. prolifera* releases DMSP throughout its lifecycle,[53] with concentrations during decay 2−3 times higher than during growth (Figure S14).[54] This parallels the 2−3 fold increase in CH_4 flux observed during decay (Figure S11a). Notably, *Pseudophaeobacter*, which can degrade DMSP and produce CH_4 as a byproduct,[55,56] showed increased relative abundance during decay (Figure 6). Concurrently, DMSP lyase activity increased significantly ($p < 0.05$, Welch's ANOVA) during the decay stage (Figure S15), providing direct enzymatic evidence for microbial-mediated aerobic CH_4 production. Therefore, we infer that ROS-driven CH_4 production may predominate during macroalgal growth, while microbial degradation of DMSP dominates during decay.

In oxygenated waters, methylphosphonate (MPn) constitutes an additional important precursor for CH_4 production.[13] MPn demethylation catalyzed by C−P lyase can promote aerobic CH_4 production but it has only been verified in cyanobacteria.[4,16] Similar to certain microorganisms, cyanobacteria utilize MPn via C−P lyase under P-deficient conditions. This process not only provides inorganic PO_4^{3-} required for microbial or algal growth, but also releases CH_4 as a byproduct through demethylation.[57] Although macroalgae cannot directly utilize MPn like cyanobacteria, macroalgae-derived organic matter (especially polysaccharides) may contain some MPn,[4,18] providing precursors for methanogenesis. Here, different PO_4^{3-} addition experiments revealed an inverse relationship between PO_4^{3-} availability and CH_4 release (Figures 4c and S7a). Fourier transform infrared (FTIR) spectroscopy revealed accumulation of C−P bonds in macroalgal-derived organic matter (Figure S16), suggesting the release of MPn by macroalgae. Concurrently, MPn levels declined more sharply under low PO_4^{3-} conditions (1.25 μM vs 0.56 μM, Figure S7b), suggesting its enhanced microbial utilization under PO_4^{3-} limitation. We also observed increased relative abundance of *Rhodobacteraceae* (known C−P lyase utilizers)[13] (Figure 6b) and elevated C−P lyase activity during decay (Figure S17). These results collectively demonstrate microbially mediated MPn demethylation as a source of aerobic CH_4 production by macroalgae. Indeed, day 5 marks a clear transition between the growth and decay stages in our cultivations (Figure S2a). The reduced DO levels coupled with the accumulation of methanogenic precursors (i.e., DMSP and MPn) contribute to the elevated CH_4 emissions observed during macroalgal decay.

Methanogenic archaea survive via anoxic microniches: Despite sustained oxygenated conditions in the bulk seawater (Figure S12), methanogenic archaea, including *Methanobrevibacter*, *Methanosaeta*, *Methanolobus*, *Methanosarcina*, and *Methanobacterium*, were detected throughout the cultivation of *U. prolifera* (but were not detected in controls), especially

https://doi.org/10.1021/acs.est.5c18290
Environ. Sci. Technol. XXXX, XXX, XXX−XXX

during decay (Figure S10a). This apparent paradox is resolved by algal biomass aggregation and algal-derived detritus or POC accumulation, which create transient anoxic microniches in oxygenated waters.[15] During vigorous macroalgal growth, photosynthetic oxygen supersaturation likely suppresses archaeal activity. In contrast, decaying macroalgae exhibits diminished photosynthetic activity (Figure S2), reduced DO levels (Figure S12a), and enhanced organic matter release (Figure S3), collectively fostering archaeal methanogenesis via CO_2 acetate and methylated compounds.[58] Direct evidence supporting this mechanism was the detection of hypoxic microenvironments (DO < 2 mg/L) deep within the macroalgal matrix (Figure S18). Notably, DO levels within these microniches decreased sharply with increasing biomass density: from 3.80 ± 0.10 mg/L at 1 g *fw*/L to 0.55 ± 0.12 at 10 g *fw*/L (Table S2). This density-dependent oxygen depletion corresponded with a 1.8 to 2.4 fold increase in maximum CH_4 emission flux at higher macroalgal densities (5 and 10 g/L) compared to the lowest density (1 g/L) (Figure S11a), underscoring a clear density-dependent enhancement of methanogenesis. Thus, the microniche hypothesis provides a coherent mechanism reconciling the coexistence of bulk aerobic conditions with localized anaerobic CH_4 production.

Overall, CH_4 production in oxygenated macroalgal systems is driven by three complementary pathways: (1) direct nonenzymatic CH_4 release via photosynthetic and ROS-mediated demethylation of methylated sulfur compounds; (2) microbial degradation of algal-derived precursors such as DMSP and MPn; and (3) archaeal methanogenesis within localized anoxic microniches. Together, these mechanisms establish macroalgae as previously unrecognized but significant sources of CH_4 in aerobic marine waters.

In marine ecosystems, ammonia oxidation and denitrification represent the primary pathways of N_2O production.[24] While conventional understanding assigns ammonia oxidation dominance in oxygenated waters and denitrification prevalence in anoxic zones,[23] emerging evidence challenges this dichotomous paradigm. Aggregated particulate organic matter generates low DO microniches that expand habitats for denitrifier, allowing them to contribute substantially to N_2O production even in oxygenated environments.[3] During our cultivations, anoxic niches detected deep within the macroalgal matrix support denitrification potential under ostensibly aerobic conditions (Figure S18). Moreover, isotopic tracing experiment unequivocally confirmed dual production pathways for N_2O production, with $^{15}N_2O$ accumulation observed in both $^{15}NH_4^+$ and $^{15}NO_3^-$ amended treatments (Figure 5), indicating concurrent ammonia oxidation and denitrification in aerobic waters (Figure S19). Field metatranscriptomics of green tides corroborate this coupling, showing sustained coexpression of ammonia oxidation genes (amoABC/nxrAB) and denitrification genes (nirK/nirS).[59] This transcriptional coordination establishes mechanistic evidence for oxygen gradient-driven niche partitioning within macroalgal aggregates.[3,60] Notably, $^{15}N_2O$ concentrations in the $^{15}NO_3^-$ group were significantly higher than that in the $^{15}NH_4^+$ group during the first 5 days but declined thereafter (Figure 5). This decrease coincided with the depletion of NO_3^- (Figure S20b), whereas NH_4^+ concentration initially decreased rapidly and then stabilized at ∼2 μM until the end (Figure S20a). These results suggest that NO_3^- availability may be a key factor controlling N_2O production, and that denitrification dominates N_2O generation under nitrate-replete conditions even in aerobic environments (Figures 5, S19 and S20). Microbial community analysis showed enriched denitrification-associated taxa (e.g., *Saprospiraceae*, *Arcobacteraceae* and *Nitrincolaceae*) during peak N_2O production (Figures 4b and S9),[61,62] supporting this inference. In coastal environments, NO_3^- is often the dominant DIN species (>90%), hence denitrification may be the main pathway for N_2O production in macroalgal ecosystems under eutrophic conditions. During decay, N_2O production declined to negligible levels (Figure 2b), concurrent with *N*-nutrient depletion (Figure S6a−c). It is noteworthy that under future eutrophication scenarios characterized by elevated N/P ratios, the multiple production pathways of CH_4 and N_2O identified in this study may amplify the climate forcing of macroalgal ecosystems. Such stoichiometric imbalance could exert multiple effects: (i) promoting denitrification-dominated N_2O production during active macroalgal growth, and (ii) inducing phosphorus limitation that triggers MPn-mediated methanogenesis during senescence. The ongoing shifts in coastal nutrient stoichiometry may influence the non-CO_2 climate footprint of macroalgal ecosystems, underscoring the need to integrate nutrient dynamics into assessments of their net climate impacts.

During the cultivation of *U. prolifera*, microbial community structure underwent significant succession and exhibited distinct stage-dependent responses (Figures 6 and S9). Taxa specialized in the degradation of macroalgal-derived organic carbon, particularly the bacterial classes *Bacteroidia* and *Clostridia*, showed markedly higher abundance during decay than during growth (Figure 6a). This temporal variation correlated with the increased release of POC and DOC during macroalgal senescence (Figure S3), consistent with previous observations in macroalgal degradation systems.[21,63] Meanwhile, we observed a rise in the abundance of methylotrophic bacteria involved in methanogenic pathways. Specifically, *unclassified_f_Rhodobacteraceae* and *Pseudophaeobacter*, both implicated in DMSP cleavage and MPn utilization,[11,64−66] showed pronounced proliferation during decay (Figures 6b and S9). These results provided a microbiological basis for the elevated CH_4 fluxes observed during macroalgal decay. In converse, the growth stage exhibited distinct N-cycling dynamics. Under N-replete conditions, we detected increased abundance of microbes associated with N_2O production, including *Saprospiraceae*, *Arcobacteraceae*, *Nitrincolaceae*, uncategorized *Nitrosopumilaceae*, *Nitrososphaeraceae*, *Nitrosotaleaceae* (Figures S9 and S10b). Their temporal synchronization with algal nutrient assimilation suggests active microbial mediation of N transformations, ultimately driving N_2O emissions during active biomass accumulation.[62,67]

U. prolifera has caused the world's largest green tide in the Yellow Sea annually for 19 consecutive years, with each episode introducing over 5 million tons of biomass into surface seawater. While previous studies have emphasized the role of *U. prolifera* in long-term carbon sequestration through substantial CO_2 assimilation and the release of recalcitrant organic carbon (recalcitrant POC: 24% of macroalgal POC; recalcitrant DOC: 54% of macroalgal DOC),[22,32] this study reveals that it also emits substantial quantities of CH_4 and N_2O under aerobic conditions. Under environmentally representative conditions (macroalgal density: 3 g/L, NO_3^-: 20 μM, PO_4^{3-}: 1.25 μM), the daily fluxes of CH_4 and N_2O released by *U. prolifera* reached 3.8 ± 1.3 mg m^{-2} d^{-1} and 0.13 ± 0.06 mg m^{-2} d^{-1} (Figure 7). Based on the maximum recorded coverage (2262 km^2) of green tide in the Yellow Sea during 2023,[68] we

https://doi.org/10.1021/acs.est.5c18290
Environ. Sci. Technol. XXXX, XXX, XXX−XXX

estimate that floating macroalgae can release up to 8.6 kg CH_4 and 0.29 kg N_2O into the atmosphere per day. It is important to note that natural coastal environments are more complex than controlled laboratory settings. Physical factors such as wind speed and wave conditions can substantially modulate in situ gas emissions. Wind speed directly governs the gas transfer velocity (k) across the air-sea interface,[39,40] with elevated wind speeds proportionally enhancing instantaneous emission fluxes (eq 2). Wave conditions, closely coupled with wind forcing, further influence emissions by enhancing near-surface turbulence and gas exchange efficiency.[40] In addition, wave action may alter the physical configuration of floating macroalgal mats, potentially affecting the formation and persistence of anoxic microenvironments within the macroalgal matrix. Under high-wind and high-wave conditions associated with the summer monsoon in the Yellow Sea (maximum wind speeds of 10 m s^{-1}, maximum wave heights of 2.8 m),[69,70] actual CH_4 and N_2O emissions from *U. prolifera* green tides may substantially differ with our laboratory-derived estimates. These possibilities underscore the need for future field-based flux measurements that capture the influence of dynamic environmental conditions on greenhouse gas emissions in macroalgal ecosystems.

Coastal vegetated ecosystems are recognized global CH_4 emission hotspots, with mangroves (0.34 Tg CH_4 yr^{-1}) > salt marshes (0.26 Tg CH_4 yr^{-1}) > seagrasses (0.17 Tg CH_4 yr^{-1}), collectively releasing 0.76 Tg CH_4 yr^{-1}, more than three times that of global estuaries.[71] While mangrove CH_4 emissions are primarily driven by carbon-rich deep anoxic sediments and tidally mediated advection of CH_4-enriched groundwater,[72] macroalgal ecosystems are dominated by aerobic methanogenesis. In the Baltic Sea, macroalgal ecosystems exhibit atmospheric CH_4 effluxes of 0.1−2.9 mg CH_4 m^{-2} d^{-1}, offsetting 28% of their CO_2 sequestration capacity over annual cycles.[14] This large carbon-climate trade-off underscores the necessity of incorporating aerobic methanogenesis into future assessments of the net climate effect of macroalgae.

In conclusion, our study establishes marine macroalgae as previously unrecognized but substantial sources of CH_4 and N_2O in aerobic marine environments, providing new insights into their role in marine climate regulation. Notably, beyond *U. prolifera*, other bloom-forming and widely distributed macroalgae, such as *Sargassum*, kelp (e.g., *Ecklonia radiata*), and *Gracilaria*, are also known to produce methanogenic precursors such as DMSP,[73,74] and likely possess aerobic methanogenesis mechanisms similar to those observed in *U. prolifera*. This suggests that aerobic CH_4 and N_2O production could be a widespread trait among macroalgae, with potential implications for coastal greenhouse gas budgets across diverse macroalgal ecosystems. Accordingly, future assessments of the biogeochemical and climatic significance of macroalgal ecosystems must integrate both carbon sequestration potential and emissions of non-CO_2 greenhouse gases to fully evaluate their net climate feedback.

■ ASSOCIATED CONTENT

Supporting Information

The Supporting Information is available free of charge at https://pubs.acs.org/doi/10.1021/acs.est.5c18290.

Supporting materials and methods, including detailed descriptions of the sample collection and analysis; additional figures and tables including heatmap analysis; dynamic changes in F_v/F_m of *U. prolifera*; DOC, POC, and DIC concentrations; NO_3^-, NO_2^-, NH_4^+, PO_4^{3-} and MPn concentrations; pH and DMSP concentrations; CH_4 and N_2O emissions fluxes; ROS content in *U. prolifera*; scatter plots between CH_4 concentrations and ROS content; DO concentrations and horizontal profiles of DO within the macroalgal matrix; microbial abundance, microbial community structure at the family level and the sequencing results; DMSP lyase and C−P lyase activities; Fourier transform infrared (FTIR) spectroscopy of *U. prolifera*-derived organic matter during the cultivation of *U. prolifera*; and in situ concentrations of DOC, POC, DIC, microbial abundance and environmental parameters in massive-macroalgae and none-macroalgae areas (PDF)

■ AUTHOR INFORMATION

Corresponding Authors

Liyang Zhan − *Key Laboratory of Global Change and Marine-Atmospheric Chemistry, Third Institute of Oceanography, Ministry of Natural Resources, Xiamen 361005, China*; Email: zhanliyang@tio.org.cn

Yongyu Zhang − *Qingdao New Energy Shandong Laboratory, Shandong Energy Institute Qingdao Institute of Bioenergy and Bioprocess Technology, Chinese Academy of Sciences, Qingdao 266101, China; University of Chinese Academy of Sciences, Beijing 100049, China*; orcid.org/0000-0002-5065-1237; Email: zhangyy@qibebt.ac.cn

Authors

Hongmei Li − *Qingdao New Energy Shandong Laboratory, Shandong Energy Institute Qingdao Institute of Bioenergy and Bioprocess Technology, Chinese Academy of Sciences, Qingdao 266101, China; University of Chinese Academy of Sciences, Beijing 100049, China; Frontiers Science Center for Deep Ocean Multispheres and Earth System, and Key Laboratory of Marine Chemistry Theory and Technology, Ministry of Education, Ocean University of China, Qingdao 266102, China*

Xiaojie Wang − *Qingdao New Energy Shandong Laboratory, Shandong Energy Institute Qingdao Institute of Bioenergy and Bioprocess Technology, Chinese Academy of Sciences, Qingdao 266101, China; University of Chinese Academy of Sciences, Beijing 100049, China*

Yue Tian − *Qingdao New Energy Shandong Laboratory, Shandong Energy Institute Qingdao Institute of Bioenergy and Bioprocess Technology, Chinese Academy of Sciences, Qingdao 266101, China; School of Environmental & Municipal Engineering, Qingdao University of Technology, Qingdao 266520, China*

Xianhui Wan − *College of Ocean and Earth Sciences, State Key Laboratory of Marine Environmental Science, Xiamen University, Xiamen 361101, China*; orcid.org/0000-0002-4870-7369

Zenghu Zhang − *Qingdao New Energy Shandong Laboratory, Shandong Energy Institute Qingdao Institute of Bioenergy and Bioprocess Technology, Chinese Academy of Sciences, Qingdao 266101, China; University of Chinese Academy of Sciences, Beijing 100049, China*

Yihua Xiao − *School of Environmental & Municipal Engineering, Qingdao University of Technology, Qingdao 266520, China*

https://doi.org/10.1021/acs.est.5c18290
Environ. Sci. Technol. XXXX, XXX, XXX−XXX

Complete contact information is available at:
https://pubs.acs.org/10.1021/acs.est.5c18290

Author Contributions

[¶]H. L., X. W. and Y. T. are contributed equally to this work.

Notes

The authors declare no competing financial interest.

■ ACKNOWLEDGMENTS

This work was supported by the National Key Research and Development Project of China (2023YFE0113102), Southern Marine Science and Engineering Guangdong Laboratory (Zhuhai) (SML2023SP218), the NSFC projects (No. 42576034, 42176050, U1906216), the National Key Research and Development project of China (2020YFA0608304), the Qingdao New Energy Shandong Laboratory Open Project (QNESL OP202306), the Youth Innovation Promotion Association of the CAS (2022208), the Shandong Distinguished Young Scholar Fund (ZR2024YQ042), the Taishan Scholars/Industrial Experts Program of Shandong Province (tsqn202312270, tsqn202408283, tscy20241145), and the Ocean Negative Carbon Emissions (ONCE) Project.

■ REFERENCES

(1) Eyre, B. D.; Camillini, N.; Glud, R. N.; Rosentreter, J. A. The climate benefit of seagrass blue carbon is reduced by methane fluxes and enhanced by nitrous oxide fluxes. *Commun. Earth Environ.* **2023**, *4*, 374.

(2) *IPCC, Climate Change 2023: Synthesis Report. Contribution of Working Groups I, II and III to the Sixth Assessment Report of the Intergovernmental Panel on Climate Change in Core Writing Team*; Lee, H., Romero, J., Eds.; IPCC, 2023

(3) Wan, X. S.; Sheng, H.-X.; Dai, M.; Casciotti, K. L.; Church, M. J.; Zou, W.; Liu, L.; Shen, H.; Zhou, K.; Ward, B. B.; Kao, S.-J. Epipelagic nitrous oxide production offsets carbon sequestration by the biological pump. *Nat. Geosci.* **2023**, *16*, 29−36.

(4) Mao, Y.; Lin, T.; Li, H.; He, R.; Ye, K.; Yu, W.; He, Q. Aerobic methane production by phytoplankton as an important methane source of aquatic ecosystems: Reconsidering the global methane budget. *Sci. Total Environ.* **2024**, *907*, 167864.

(5) Saderne, V.; Dunne, A. F.; Rich, W. A.; Cadiz, R.; Carvalho, S.; Cúrdia, J.; Kattan, A. Seasonality of methane and carbon dioxide emissions in tropical seagrass and unvegetated ecosystems. *Commun. Earth Environ.* **2023**, *4*, 99.

(6) Pan, H.; Zhou, Z.; Zhang, S.; Wang, F.; Wei, J. N_2O emissions from aquatic ecosystems: A review. *Atmosphere* **2023**, *14*, 1291.

(7) Li, H. M.; Zhang, Z. H.; Xiong, T. Q.; Tang, K. X.; He, C.; Shi, Q.; Jiao, N. Z.; Zhang, Y. Y. Carbon sequestration in the form of recalcitrant dissolved organic carbon in a seaweed (Kelp) farming environment. *Environ. Sci. Technol.* **2022**, *56*, 9112−9122.

(8) Duarte, C. M.; Delgado-Huertas, A.; Marti, E.; Gasser, B.; Martin, I. S.; Cousteau, A.; Neumeyer, F.; Reilly-Cayten, M.; Boyce, J.; Kuwae, T.; Hori, M.; Miyajima, T.; Price, N. N.; Arnold, S.; Ricart, A. M.; Davis, S.; Surugau, N.; Abdul, A.-J.; Wu, J.; Xiao, X.; Chung, I. K.; Choi, C. G.; Sondak, C. F. A.; Albasri, H.; Krause-Jensen, D.; Bruhn, A.; Boderskov, T.; Hancke, K.; Funderud, J.; Borrero-Santiago, A. R.; Pascal, F.; Joanne, P.; Ranivoarivelo, L.; Collins, W. T.; Clark, J.; Gutierrez, J. F.; Riquelme, R.; Avila, M.; Macreadie, P. I.; Masque, P. Carbon burial in sediments below seaweed farms matches that of Blue Carbon habitats. *Nat. Clim. Change* **2025**, *15*, 180−187.

(9) Filbee-Dexter, K.; Pessarrodona, A.; Pedersen, M. F.; Wernberg, T.; Duarte, C. M.; Assis, J.; Bekkby, T.; Burrows, M. T.; Carlson, D. F.; Gattuso, J.-P.; Gundersen, H.; Hancke, K.; Krumhansl, K. A.; Kuwae, T.; Middelburg, J. J.; Moore, P. J.; Queirós, A. M.; Smale, D. A.; Sousa-Pinto, I.; Suzuki, N.; Krause-Jensen, D. Carbon export from seaweed forests to deep ocean sinks. *Nat. Geosci.* **2024**, *17*, 552−559.

(10) Simpkins, T.; Van der Mheen, M.; Pedersen, M.; Pessarrodona, A.; Pattiaratchi, C.; Wernberg, T.; Filbee-Dexter, K. Macroalgae detritus decomposition and cross-shelf carbon export from shallow and deep reefs. *Limnol. Oceanogr.* **2025**, *70*, 1046−1058.

(11) Ye, W.; Wang, X.; Zhang, X.-H.; Zhang, G. Methane production in oxic seawater of the western North Pacific and its marginal seas. *Limnol. Oceanogr.* **2020**, *65*, 2352−2365.

(12) Wang, Y.; Feng, M.; Wang, J.; Chen, X.; Chen, X.; Du, X.; Xun, F.; Ngwenya, B. T. Algal blooms modulate organic matter remineralization in freshwater sediments: A new insight on priming effect. *Sci. Total Environ.* **2021**, *784*, 147087.

(13) von Arx, J. N.; Kidane, A. T.; Philippi, M.; Mohr, W.; Lavik, G.; Schorn, S.; Kuypers, M. M. M.; Milucka, J. Methylphosphonate-driven methane formation and its link to primary production in the oligotrophic North Atlantic. *Nat. Commun.* **2023**, *14*, 6529.

(14) Roth, F.; Broman, E.; Sun, X.; Bonaglia, S.; Nascimento, F.; Prytherch, J.; Brüchert, V.; Lundevall Zara, M.; Brunberg, M.; Geibel, M. C.; Humborg, C.; Norkko, A. Methane emissions offset atmospheric carbon dioxide uptake in coastal macroalgae, mixed vegetation and sediment ecosystems. *Nat. Commun.* **2023**, *14*, 42.

(15) Ye, J.; Zhuang, M.; Hong, M.; Zhang, D.; Ren, G.; Hu, A.; Yang, C.; He, Z.; Zhou, S. Methanogenesis in the presence of oxygenic photosynthetic bacteria may contribute to global methane cycle. *Nat. Commun.* **2024**, *15*, 5682.

(16) Ernst, L.; Steinfeld, B.; Barayeu, U.; Klintzsch, T.; Kurth, M.; Grimm, D.; Dick, T. P.; Rebelein, J. G.; Bischofs, I. B.; Keppler, F. Methane formation driven by reactive oxygen species across all living organisms. *Nature* **2022**, *603*, 482−487.

(17) Rao, Y.; Gao, G.; Berman-Frank, I.; Bizic, M.; Gao, K. Light-dependent methane production by a coccolithophorid may counteract its photosynthetic contribution to carbon dioxide sequestration. *Commun. Earth Environ.* **2024**, *5*, 695.

(18) Repeta, D. J.; Ferrón, S.; Sosa, O. A.; Johnson, C. G.; Repeta, L. D.; Acker, M.; DeLong, E. F.; Karl, D. M. Marine methane paradox explained by bacterial degradation of dissolved organic matter. *Nat. Geosci.* **2016**, *9*, 884−887.

(19) Mao, S.-H.; Zhang, H.-H.; Zhuang, G.-C.; Li, X.-J.; Liu, Q.; Zhou, Z.; Wang, W.-L.; Li, C.-Y.; Lu, K.-Y.; Liu, X.-T.; Montgomery, A.; Joye, S. B.; Zhang, Y.-Z.; Yang, G.-P. Aerobic oxidation of methane significantly reduces global diffusive methane emissions from shallow marine waters. *Nat. Commun.* **2022**, *13*, 7309.

(20) Hall, N.; Wong, W. W.; Lappan, R.; Ricci, F.; Jeppe, K. J.; Glud, R. N.; Kawaichi, S.; Rotaru, A. E.; Greening, C.; Cook, P. L. M. Coastal methane emissions driven by aerotolerant methanogens using seaweed and seagrass metabolites. *Nat. Geosci.* **2025**, *18*, 854−861.

(21) Chen, J.; Li, H. M.; Zhang, Z. H.; He, C.; Shi, Q.; Jiao, N. Z.; Zhang, Y. Y. DOC dynamics and bacterial community succession during long-term degradation of *Ulva prolifera* and their implications for the legacy effect of green tides on refractory DOC pool in seawater. *Water Res.* **2020**, *185*, 116268.

(22) Li, H. M.; Feng, X. T.; Xiong, T. Q.; Shao, W.; Wu, W. C.; Zhang, Y. Y. Particulate organic carbon released during macroalgal growth has significant carbon sequestration potential in the ocean. *Environ. Sci. Technol.* **2023**, *57*, 19723−19731.

(23) Wan, X. S.; Hou, L.; Kao, S.-J.; Zhang, Y.; Sheng, H.-X.; Shen, H.; Tong, S.; Qin, W.; Ward, B. B. Pathways of N_2O production by marine ammonia-oxidizing archaea determined from dual-isotope labeling. *Proc. Natl. Acad. Sci.* **2023**, *120*, No. e2220697120.

(24) Wan, X. S.; Sheng, H.-X.; Liu, L.; Shen, H.; Tang, W.; Zou, W.; Xu, M. N.; Zheng, Z.; Tan, E.; Chen, M.; Zhang, Y.; Ward, B. B.; Kao, S.-J. Particle-associated denitrification is the primary source of N_2O in oxic coastal waters. *Nat. Commun.* **2023**, *14*, 8280.

(25) Wang, S.; Huang, J.; Wu, Z.; Li, S.; Zhu, X.; Liu, Y.; Ji, G. Global mapping of flux and microbial sources for oceanic N_2O. *Nat. Commun.* **2025**, *16*, 3341.

(26) Yao, Y.; Chen, Y.; Han, R.; Chen, D.; Ma, H.; Han, X.; Feng, Y.; Shi, C. Algal decomposition accelerates denitrification as evidenced by the high-resolution distribution of nitrogen fractions

in the sediment−water interface of eutrophic lakes. *Water* **2024**, *16*, 341.
(27) Zhou, Y.; Xu, X.; Song, K.; Yeerken, S.; Deng, M.; Li, L.; Riya, S.; Wang, Q.; Terada, A. Nonlinear pattern and algal dual-impact in N_2O emission with increasing trophic levels in shallow lakes. *Water Res.* **2021**, *203*, 117489.
(28) Dai, M.; Zhao, Y.; Chai, F.; Chen, M.; Chen, N.; Chen, Y.; Cheng, D.; Gan, J.; Guan, D.; Hong, Y.; Huang, J.; Lee, Y.; Leung, K.; Lim, P. E.; Lin, S.; Lin, X.; Liu, X.; Liu, Z.; Luo, Y.-W.; Meng, F.; et al. Persistent eutrophication and hypoxia in the coastal ocean. *Camb. Prism. Coast. Futur.* **2023**, *1*, No. e19.
(29) Xiong, T. Q.; Li, H. M.; Yue, Y. F.; Hu, Y. B.; Zhai, W. D.; Xue, L.; Jiao, N. Z.; Zhang, Y. Y. Legacy effects of late macroalgal blooms on dissolved inorganic carbon pool through alkalinity enhancement in coastal ocean. *Environ. Sci. Technol.* **2023**, *57*, 2186−2196.
(30) Li, H.-M.; Zhang, C.-S.; Han, X.-R.; Shi, X.-Y. Changes in concentrations of oxygen, dissolved nitrogen, phosphate, and silicate in the southern Yellow Sea, 1980−2012: Sources and seaward gradients. *Estuar. Coast. Shelf Sci.* **2015**, *163*, 44−55.
(31) Ye, W.; Li, Y.; Wen, J.; Zhang, J.; Shakhova, N.; Liu, J.; Wu, M.; Semiletov, I.; Zhan, L. Enhanced transport of dissolved methane from the Chukchi Sea to the central arctic. *Global Biogeochem. Cycles* **2023**, *37*..
(32) Li, H.; Feng, X.; Xiong, T.; He, C.; Wu, W.; Shi, Q.; Jiao, N.; Zhang, Y. Green tides significantly alter the molecular composition and properties of coastal DOC and perform dissolved carbon sequestration. *Environ. Sci. Technol.* **2023**, *57*, 770−779.
(33) Li, H.; Zhang, Y.; Chen, J.; Zheng, X.; Liu, F.; Jiao, N. Nitrogen uptake and assimilation preferences of the main green tide alga *Ulva prolifera* in the Yellow Sea, China. *J. Appl. Phycol.* **2019**, *31*, 625−635.
(34) Xu, J.; Zhao, X.; Zhong, Y.; Qu, T.; Sun, B.; Zhang, H.; Hou, C.; Zhang, Z.; Tang, X.; Wang, Y. Acclimation of intertidal macroalgae *Ulva prolifera* to UVB radiation: the important role of alternative oxidase. *BMC Plant Biol.* **2024**, *24*, 143.
(35) Guo, Y.-Y.; Li, T.; Cao, X.-Y.; Zhu, M.-X. Effective capping of dissolved sulfide generated in *Ulva prolifera*-rich marine sediments by iron-rich red soil. *Mar. Pollut. Bull.* **2024**, *203*, 116424.
(36) Xu, N.; Tan, G.; Wang, H.; Gai, X. Effect of biochar additions to soil on nitrogen leaching, microbial biomass and bacterial community structure. *Eur. J. Soil Biol.* **2016**, *74*, 1−8.
(37) Wu, K.; Zhou, L.; Tahon, G.; Liu, L.; Li, J.; Zhang, J.; Zheng, F.; Deng, C.; Han, W.; Bai, L.; Fu, L.; Dong, X.; Zhang, C.; Ettema, T. J. G.; Sousa, D. Z.; Cheng, L. Isolation of a methyl-reducing methanogen outside the Euryarchaeota. *Nature* **2024**, *632*, 1124−1130.
(38) Wiesenburg, D. A.; Guinasso, N. L., Jr Equilibrium solubilities of methane, carbon monoxide, and hydrogen in water and sea water. *J. Chem. Eng. Data* **1979**, *24*, 356−360.
(39) Wanninkhof, R. Relationship between wind speed and gas exchange over the ocean. *J. Geophys. Res., Oceans* **1992**, *97*, 7373−7382.
(40) Wanninkhof, R. Relationship between wind speed and gas exchange over the ocean revisited. *Limnol. Oceanogr. Methods* **2014**, *12*, 351−362.
(41) Feng, L. N.; Zhang, H. B.; Sun, Y. Y.; Li, X. Z.; Su, R. G.; Shi, X. Y. On nutrient releases from the decomposition of *Ulva prolifera* green tide and their impacts on nearshore seawaters in the southern Yellow Sea. *Haiyang Xuebao* **2020**, *42*, 59−68.
(42) Liu, X. Q. *Distributions of Floating Green Algae and Micro-propagules in the Formatting and Developing Processes in the Yellow Sea*; Liu, X. Q., Ed.; First Institute of Oceanography, State Oceanic Administration, 2014; .
(43) Feehan, C. J. *Seaweed farming: Assessment on the potential of sustainable upscaling for climate, communities and the planet*; United Nations Environment Programme (UNEP). 2023
(44) Ross, F. W. R.; Boyd, P. W.; Filbee-Dexter, K.; Watanabe, K.; Ortega, A.; Krause-Jensen, D.; Lovelock, C.; Sondak, C. F. A.; Bach, L. T.; Duarte, C. M.; Serrano, O.; Beardall, J.; Tarbuck, P.; Macreadie, P. I. Potential role of seaweeds in climate change mitigation. *Sci. Total Environ.* **2023**, *885*, 163699.
(45) Zhai, X.; Li, J.; Zhang, H.; Tan, D.; Yang, G. Spatial distribution and biogeochemical cycling of dimethylated sulfur compounds and methane in the East China Sea during spring. *J. Geophys. Res., Oceans.* **2019**, *124*, 1074−1090.
(46) Zhang, Y.; Tan, D.; He, Z.; Yu, J.; Yang, G. Dimethylated sulfur, methane and aerobic methane production in the Yellow Sea and Bohai Sea. *J. Geophys. Res., Oceans* **2023**, *128*, No. e2023JC019736.
(47) Li, C.; Wang, X.; Chen, X.; Sheng, Q.; Zhang, S.; Wang, P.; Quareshy, M.; Rihtman, B.; Shao, X.; Gao, C.; Li, F.; Li, S.; Zhang, W.; Zhang, X.; Yang, G.; Todd, J. D.; Chen, Y.; Zhang, Y. A novel ATP dependent dimethylsulfoniopropionate lyase in bacteria that releases dimethyl sulfide and acryloyl-CoA. *eLife* **2021**, *10*, No. e64045.
(48) Shaw, D. K.; Sekar, J.; Ramalingam, P. V. Recent insights into oceanic dimethylsulfoniopropionate biosynthesis and catabolism. *Environ. Microbiol.* **2022**, *24*, 2669−2700.
(49) Han, L.; Xin, Y.; Wang, J.; Li, P.-F.; Liu, T.; Duan, S.-S.; Liu, C.-Y.; Yang, G.-P. Sulfur metabolism and response to light in *Ulva prolifera* green tides. *Environ. Pollut.* **2025**, *366*, 125523.
(50) Shemi, A.; Alcolombri, U.; Schatz, D.; Farstey, V.; Vincent, F.; Rotkopf, R.; Ben-Dor, S.; Frada, M. J.; Tawfik, D. S.; Vardi, A. Dimethyl sulfide mediates microbial predator−prey interactions between zooplankton and algae in the ocean. *Nat. Microbiol.* **2021**, *6*, 1357−1366.
(51) Bižić, M.; Klintzsch, T.; Ionescu, D.; Hindiyeh, M. Y.; Günthel, M.; Muro-Pastor, A. M.; Eckert, W.; Urich, T.; Keppler, F.; Grossart, H. P. Aquatic and terrestrial cyanobacteria produce methane. *Sci. Adv.* **2020**, *6*, No. eaax5343.
(52) Hilt, S.; Grossart, H.-P.; McGinnis, D.; Keppler, F. Potential role of submerged macrophytes for oxic methane production in aquatic ecosystems. *Limnol. Oceanogr.* **2022**, *67*, S76−S88.
(53) Zhang, X.; Liu, J.; Liu, J.; Yang, G.; Xue, C.; Curson, A. R. J.; Todd, J. D. Biogenic production of DMSP and its degradation to DMS their roles in the global sulfur cycle. *Sci. China Life Sci.* **2019**, *62*, 1296−1319.
(54) Han, L.; Yang, G.; Liu, C.; Jin, Y.; Liu, T. Emissions of biogenic sulfur compounds and their regulation by nutrients during an *Ulva prolifera* bloom in the Yellow Sea. *Mar. Pollut. Bull.* **2021**, *162*, 111885.
(55) Damm, E.; Thoms, S.; Beszczynska-Möller, A.; Nöthig, E. M.; Kattner, G. Methane excess production in oxygen-rich polar water and a model of cellular conditions for this paradox. *Polar Sci.* **2015**, *9*, 327−334.
(56) Liu, J.; Xue, C.; Wang, J.; Crombie, A.; Carrion, O.; Johnston, A.; Murrell, J.; Liu, J.; Zheng, Y.; Zhang, X.; Todd, J. *Oceanospirillales* containing the DMSP lyase DddD are key utilisers of carbon from DMSP in coastal seawater. *Microbiome* **2022**, *10*, 110.
(57) Peoples, L. M.; Dore, J. E.; Bilbrey, E. M.; Vick-Majors, T. J.; Ranieri, J. R.; Evans, K. A.; Ross, A. M.; Devlin, S. P.; Church, M. J. Oxic methane production from methylphosphonate in a large oligotrophic lake: limitation by substrate and organic carbon supply. *Appl. Environ. Microbiol.* **2023**, *89*, No. e01097-23.
(58) Söllinger, A.; Urich, T. Methylotrophic methanogens everywhere physiology and ecology of novel players in global methane cycling. *Biochem. Soc. Trans.* **2019**, *47*, 1895−1907.
(59) Rees, A. P.; Brown, I. J.; Jayakumar, A.; Lessin, G.; Somerfield, P. J.; Ward, B. B. Biological nitrous oxide consumption in oxygenated waters of the high latitude Atlantic Ocean. *Commun. Earth Environ.* **2021**, *2*, 36.
(60) Klawonn, I.; Bonaglia, S.; Brüchert, V.; Ploug, H. Aerobic and anaerobic nitrogen transformation processes in N_2-fixing cyanobacterial aggregates. *ISME J.* **2015**, *9*, 1456−1466.
(61) Li, J.; Xiang, S.; Li, Y.; Cheng, R.; Lai, Q.; Wang, L.; Li, G.; Dong, C.; Shao, Z. Arcobacteraceae are ubiquitous mixotrophic bacteria playing important roles in carbon, nitrogen, and sulfur cycling in global oceans. *mSystems* **2024**, *9*, No. e00513-24.

https://doi.org/10.1021/acs.est.5c18290
Environ. Sci. Technol. XXXX, XXX, XXX−XXX

(62) Shan, H.; Du, Y.; Li, T.; Wang, F.; Li, H.; Wang, H. Bacterial community characteristics and roles in nitrogen transformation in industrial farming systems of litopenaeus vannamei. *J. Mar. Sci. Eng.* **2024**, *12*, 787.
(63) Feng, X.; Li, H.; Zhang, Z.; Xiong, T.; Shi, X.; He, C.; Shi, Q.; Jiao, N.; Zhang, Y. Microbial-mediated contribution of kelp detritus to different forms of oceanic carbon sequestration. *Ecol. Indicators.* **2022**, *142*, 109186.
(64) Zhang, S.; Cao, H. Y.; Zhang, N.; Teng, Z. J.; Yu, Y.; Wang, Z. B.; Wang, P.; Fu, H. H.; Chen, X. L.; Zhang, Y. Z.; Li, C. Y. Novel insights into dimethylsulfoniopropionate catabolism by cultivable bacteria in the Arctic Kongsfjorden. *Appl. Environ. Microbiol.* **2022**, *88*, No. e01806-21.
(65) Lin, Y.; Zhang, M.; Lai, Y.-X.; Liu, T.; Meng, M.; Sun, Y.; Wang, Y.; Dong, Q.-Y.; Li, C.-X.; Yu, M.-X.; Cheng, J.; Liu, S.-J.; Shao, X.; Zhang, N.; Li, C.-Y. Genomic analysis of Alteromonas sp. M12 isolated from the Mariana Trench reveals its role in dimethylsulfoniopropionate cycling. *Mar. Genom.* **2024**, *76*, 101112.
(66) Tout, J.; Jeffries, T. C.; Petrou, K.; Tyson, G. W.; Webster, N. S.; Garren, M.; Stocker, R.; Ralph, P. J.; Seymour, J. R. Chemotaxis by natural populations of coral reef bacteria. *ISME J.* **2015**, *9*, 1764−1777.
(67) Bellas, C. M.; Campbell, K.; Tranter, M.; Sánchez-Baracaldo, P. Nitrogen and sulfur metabolisms encoded in prokaryotic communities associated with sea ice algae. *ISME Commun.* **2023**, *3*, 131.
(68) Yu, T.; Peng, X. W.; Wang, Y.; Xu, S. W.; Liang, C.; Wang, Z. Z. Green tide cover area monitoring and prediction based on multi-source remote sensing fusion. *Mar. Pollut. Bull.* **2025**, *215*, 117921.
(69) Men, Y.; Liu, Y.; Ma, Y.; Wong, K. P.; Tsou, J. Y.; Zhang, Y. Remote sensing monitoring of green tide disaster using MODIS and GF-1 Data: A case study in the Yellow Sea. *J. Mar. Sci. Eng.* **2023**, *11*, 2212.
(70) Cao, Y.; Wu, Y.; Fang, Z.; Cui, X.; Liang, J.; Song, X. Spatiotemporal patterns and morphological characteristics of *Ulva prolifera* distribution in the Yellow Sea, China in 2016−2018. *Remote Sens.* **2019**, *11*, 445.
(71) Rosentreter, J. A.; Laruelle, G. G.; Bange, H. W.; Bianchi, T. S.; Busecke, J. J. M.; Cai, W.-J.; Eyre, B. D.; Forbrich, I.; Kwon, E. Y.; Maavara, T.; Moosdorf, N.; Najjar, R. G.; Sarma, V. V. S. S.; Van Dam, B.; Regnier, P. Coastal vegetation and estuaries are collectively a greenhouse gas sink. *Nat. Clim. Change* **2023**, *13*, 579−587.
(72) Maher, D. T.; Santos, I. R.; Golsby-Smith, L.; Gleeson, J.; Eyre, B. D. Groundwater-derived dissolved inorganic and organic carbon exports from a mangrove tidal creek: The missing mangrove carbon sink? *Limnol. Oceanogr.* **2013**, *58*, 475−488.
(73) Smit, A. J.; Robertson-Andersson, D. V.; Peall, S.; Bolton, J. J. Dimethylsulfoniopropionate (DMSP) accumulation in abalone Haliotis midae (Mollusca: Prosobranchia) after consumption of various diets, and consequences for aquaculture. *Aquaculture* **2007**, *269*, 377−389.
(74) Vila-Costa, M.; Rinta-Kanto, J. M.; Poretsky, R. S.; Sun, S.; Kiene, R. P.; Moran, M. A. Microbial controls on DMSP degradation and DMS formation in the Sargasso Sea. *Biogeochemistry* **2014**, *120*, 295−305.

https://doi.org/10.1021/acs.est.5c18290
Environ. Sci. Technol. XXXX, XXX, XXX−XXX